

Dipolar interactions induced order in assemblies of magnetic particles

R. Pastor-Satorras

*The Abdus Salam International Centre for Theoretical Physics (ICTP)
Condensed Matter Section
P.O. Box 586, 34100 Trieste, Italy*

J. M. Rubí

*Departament de Física Fonamental, Facultat de Física, Universitat de Barcelona
Diagonal 647, 08022 Barcelona, Spain*

We discuss the appearance of ordered structures in assemblies of magnetic particles. The phenomenon occurs when dipolar interactions and the thermal motion of the particles compete, and is mediated by screening and excluded volume effects. It is observed irrespective of the dimensionality of the system and the resulting structures, which may be regular or fractal, indicate that new ordered phases may emerge in these systems when dipolar interactions play a significant role.

I. INTRODUCTION

The collective behavior of assemblies of dipolar magnetic particles is governed by the influence of several competing mechanisms and presents a very rich and complex phenomenology [1] whose ultimate interest is the identification of the emerging structures and the subsequent analysis of its implications in the macroscopic properties of the system. When the particles are dispersed in an aqueous, magnetically inactive, phase, the formation of structures results—as occurs in other soft-condensed matter systems—from the interplay of dipolar interactions, excluded volume effects, and thermal motion. Unlike assemblies of non-magnetic particles, they may exhibit ordered phases emerging when dipolar interactions are dominant, and disordered phases when those interactions are inhibited by Brownian motion. In the cases of electro- and magneto-rheological dispersions, the particles are heavy enough to impede Brownian effects, and therefore chaining is the most likely event. Contrarily, for finer magnetic particles, as monodomain particles or ferrofluids, thermal motion becomes more important, opening the possibility to the analysis of the interplay with dipolar interactions, and the subsequent formation of structures. Disconnected results along this lines have been previously reported for different systems [2,3].

Our purpose in this paper is to discuss an apparent general phenomenon occurring in these systems: the emergence of order when magnetic interactions and thermal motion compete. Ordered and disordered states would then be accessible upon variation of temperature, and consequently would correspond to different structural phases of the system.

The paper is distributed as follows. In Section II we study the problem of aggregation of dipolar particles in $d = 2$ and $d = 3$, whereas in Sec. III we focus on a problem of different nature, namely the adsorption of particles onto a substrate of dimension $d = 1$ and $d = 2$. Finally, in the last Section we discuss the common features of the transition to more ordered structures when dipolar interactions play a significant role.

II. CLUSTER AGGREGATION WITH DIPOLAR INTERACTIONS

The first system we consider is the cluster aggregation of particles that experience dipolar interactions. Cluster aggregation, and in general fractal growth phenomena [4,5], are very active fields, specially in which regards the physics of colloids. In the context of computer models, the most notable are the diffusion-limited aggregation (DLA) model [6] and the cluster-cluster aggregation model [7,8], which effectively describe the fractal structure of real colloidal aggregates [9]. In this Section, we describe the extension of the standard DLA model taking into account fully anisotropic dipolar interparticle interactions.

A. Description of the algorithm

The general framework of the models we are considering is the *sequential* addition of dipolar particles of diameter a , with a moment $\boldsymbol{\mu}$ rigidly attached, to an assembly \mathcal{S} of rigid dipoles located at fixed positions. The incoming particles perform a random walk under the influence of the long-range interactions exerted by the dipoles in \mathcal{S} . The effect of these interactions is encoded in the following procedure: Consider that, at a certain time step, the structure \mathcal{S} is formed by N rigid dipoles $\boldsymbol{\mu}_i$, located at positions \mathbf{R}_i . The energy of an incoming particle of magnetic moment $\boldsymbol{\mu}$ at position \mathbf{r} , is then given by [10]

$$\mathcal{E} = \sum_{i=1}^N \frac{1}{\xi_i^3} \left\{ \boldsymbol{\mu} \cdot \boldsymbol{\mu}_i - 3 \frac{(\boldsymbol{\mu} \cdot \boldsymbol{\xi}_i)(\boldsymbol{\mu}_i \cdot \boldsymbol{\xi}_i)}{\xi_i^2} \right\}, \quad (1)$$

where $\boldsymbol{\xi}_i = \mathbf{r} - \mathbf{R}_i$ is the relative distance between particles. In the next time step, the dipole is moved to a new position $\mathbf{r}^* = \mathbf{r} + \delta\mathbf{r}$, where $\delta\mathbf{r}$ is a small increment oriented along a randomly chosen direction. The energy in the new point \mathbf{r}^* is \mathcal{E}^* , and the total variation in the energy due to the movement is $\Delta\mathcal{E} = \mathcal{E}^* - \mathcal{E}$. If $\Delta\mathcal{E} < 0$, the movement is accepted with probability 1; otherwise,

it is accepted with probability $\exp(-\Delta\mathcal{E}a^3/\mu^2T_r)$, where $T_r = a^3k_B T/\mu^2$ is a dimensionless reduced temperature, relating the intensity of the dipolar interactions μ to the actual temperature T of the system. In case of not being accepted, the trial position \mathbf{r}^* is discarded and a new one generated.

With the previous algorithm, we have taken into account the translations dynamics of the particles. For the rotational dynamics of the dipoles, we apply the following prescription: The initial orientation of the dipoles $\boldsymbol{\mu}^0$ is assigned at random. After every accepted movement, the moment of the random walker is oriented along the direction of the total magnetic force on its position. After the dipole becomes finally attached to the assembly, its moment undergoes a final relaxation, and its direction does not change any more. Indeed, this fact assumes that the relaxation time for the orientation of a particle is very short compared with the characteristic time scale of the movement of its center of mass.

The simulation of the particle-cluster aggregation process starts with a particle (the seed) located at the origin of coordinates, and bearing a randomly oriented moment $\boldsymbol{\mu}_0$. The following particles are released from a random position on a sphere of radius \mathcal{R}_{in} centered on the seed. The particles have an initial moment $\boldsymbol{\mu}_i$ assigned at random. Each particle undergoes a Brownian motion, according to the given prescription, until it either contacts the cluster or moves away a distance larger than \mathcal{R}_{out} . In this case, the particle is removed and a new one is launched. In the present simulations, we have used the values $\mathcal{R}_{\text{out}} = 2\bar{\mathcal{R}}$ and $\mathcal{R}_{\text{in}} = \mathcal{R}_{\text{out}} - 5a$, where $\bar{\mathcal{R}}$ is the radius of the cluster, measured in units of the particle diameter a . The particles stick to the cluster when they overlap one or more particles previously aggregated. The new dipole is then attached in the point of its last trajectory where it is first tangent to the surface of the cluster.

B. Numerical results in $d = 3$

Simulations of cluster aggregation of dipolar particles in $d = 3$ are extremely time-consuming. Therefore, we report only results for the limits $T_r = 0$ and $T_r = \infty$. The case $T_r = 0$ corresponds to infinitely strong dipolar interactions; the steps during the random walk are only accepted if they lower the total dipolar energy. For $T_r = \infty$ all movements are accepted and we must recover the standard DLA model [6]

In Figure 1 we show two typical clusters grown at $T_r = 0$ and $T_r = \infty$ in a box of size $L = 150a$. The growth was stopped when the radius of the clusters reached a predetermined distance to the boundary of the box. In the case $T_r = 0$, the cluster was composed by $N \sim 1500$, whereas for $T_r = \infty$ we have $N \sim 10000$. A first conclusion can be immediately drawn: At high temperatures, the clusters are more compact, having an roughly spheri-

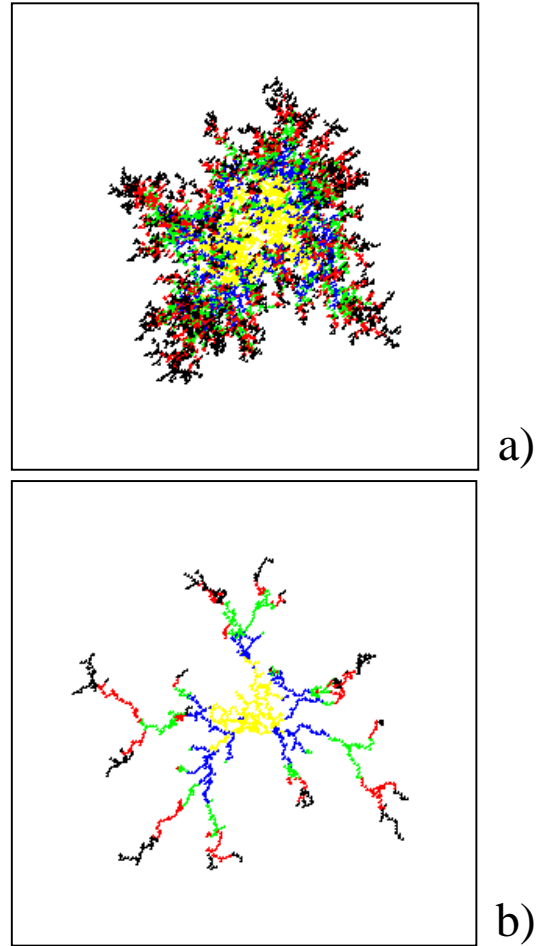


FIG. 1. Projection onto the $x-y$ plane of two typical dipolar clusters in $d = 3$, grown in a cubic box of size $L = 150a$. (a) $T_r = \infty$, $D_f = 2.47 \pm 0.03$. (b) $T_r = 0$, $D_f = 1.37 \pm 0.03$ (see text).

cal shape. When decreasing the temperature, the average density of the clusters diminishes; at $T_r = 0$, the clusters have an essentially digitated structure of very low density.

A more quantitative estimate of this concept can be obtained by measuring the fractal dimension D_f of the clusters [4]. The value of D_f is determined from a log-log plot of the radius of gyration $R_g(N)$ as a function of the number of particles in the cluster N , using the relationship [4]

$$R_g(N) = \left(\frac{1}{N} \sum_{i=1}^N R_i^2 - \frac{(\sum_{i=1}^N R_i)^2}{N^2} \right)^{1/2} \simeq N^{1/D_f}. \quad (2)$$

The value computed for the aggregation at $T_r = \infty$ is $D_f = 2.47 \pm 0.03$, in good agreement, within error bars, with the best estimate for DLA in $d = 3$, namely $D_f^{\text{DLA}} = 2.495 \pm 0.005$ [11]. On the other hand, for the simulations at zero temperature, we obtain a much smaller value, $D_f = 1.37 \pm 0.03$.

These strong variations in the structure of the cluster with temperature can be understood through a very simple and intuitive argument. The aggregation process depends on the competition between dipolar forces and thermal agitation. Dipolar interactions favor the formation of chains of aligned dipoles, thus minimizing the dipolar energy, while the thermal motion tends to randomize the process and produce a higher degree of ramification. This branching process is mediated by the *screening* of the inner regions of the cluster by the most external branches. The chances for a random walker to surpass the external active region and reach the core of the cluster are very small, and this effect induces a high branching ratio and a large fractal dimension. The balance between these two effects, branching and growth, can be measured by estimating the relative probabilities of growth, p_g , of an already existing branch and its splitting, p_s , creating thus a new branch. Assuming that the branches are composed by relaxed (parallel) dipoles, pointing along the axis of the branch, the addition of a new particle on the tip of an existing branch will increase the energy of the aggregate by an amount $\Delta\mathcal{E}_g = -2\mu^2/a^3$ (we only consider the interaction of the new particle with its nearest neighbor). We can associate to this growth event a relative probability given by a Boltzmann factor, and set $p_g = \exp(-\Delta\mathcal{E}_g a^3/\mu^2 T_r) = \exp(2/T_r)$. On the other hand, in order to minimize the energy, an incoming particle, inducing a branching event, will set its dipole antiparallel to its nearest-neighbor in the existing branch, thus increasing energy by $\Delta\mathcal{E}_s = -\mu^2/a^3$. The corresponding splitting probability is then $p_s = \exp(1/T_r)$. We have therefore

$$\frac{p_g}{p_s} = \exp(1/T_r). \quad (3)$$

At high temperature, $p_g \simeq p_s$; the growth and splitting of a given branch are equally likely events. The effect of the dipolar interactions is overcome by the thermal disorder and we must recover the original DLA with no interactions. At low temperatures, the splitting probability is vanishingly small compared with p_g , and one should expect to observe in this limit very fingered aggregates, with little branching, and a fractal dimension closer to 1, as is indeed the case in Fig. 1.

Considerations about the fractal dimension allows also to draw conclusions on the macroscopic aggregation of individual clusters. At low concentrations of dipolar particles, it is reasonable to assume that particles first form clusters, which on their hand coalesce later to form larger structures. If the mutual interactions between clusters are negligible (due to screening of the interactions in a large reservoir of clusters with random total moment) the coalescence of clusters is mediated by Brownian motion. At low temperatures, the cluster dimension is low. Let $D_f^{(1)}$ and $D_f^{(2)}$ be the fractal dimension of any two clusters in the reservoir (of course, $D_f^{(1)} = D_f^{(2)}$). Since $D_f^{(1)} + D_f^{(2)} < 3$, the clusters are transparent, have little

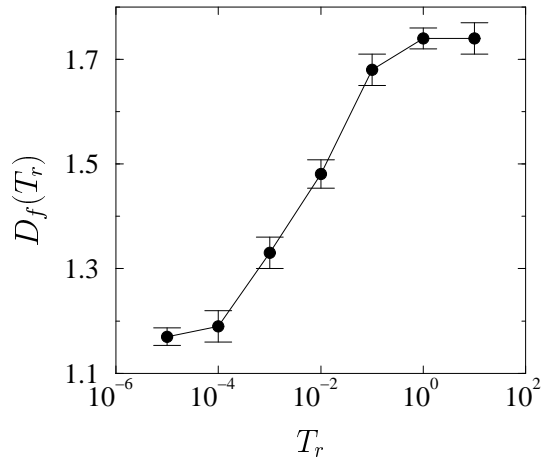


FIG. 2. Fractal dimension D_f for dipolar clusters in $d = 2$ as a function of the reduced temperature T_r .

mutual interactions and behave as essentially independent objects [12]. At high temperatures, however, the fractal dimension is larger and fulfills the condition of mutual opacity $D_f^{(1)} + D_f^{(2)} > 3$ [12]. Assuming that D_f is an increasing function of T_r (as is the case in $d = 2$, see next section), we predict the existence of a critical temperature T_r^c for which $D_f^{(1)} + D_f^{(2)} = 3$, setting the threshold above which cluster coalescence is possible, leading to the formation more complex structures.

C. Numerical results in $d = 2$

Simulations in $d = 2$ are much less costly, and afford the possibility of truly exploring the effect of temperature on the cluster structure. Moreover, simulations on a plane are also realistic and interesting on their own, because of their relevance in understanding phase transitions in Langmuir monolayers [13]. Far from equilibrium, the condensed phase grows at the expense of the liquid phase, forming clusters of different shapes. The phospholipids that make up the Langmuir monolayer experience repulsive dipolar interactions, which must play a major role in determining the morphology of the condensed aggregates.

In Figure 2 we plot the fractal dimension D_f for dipolar clusters in $d = 2$ as a function of the reduced temperature T_r . This figure confirms the arguments given in Sec. II B. At high temperatures the fractal dimension is large ($D_f = 1.74 \pm 0.03$ at $T_r = 10$) and compatible with the best estimates for free DLA ($D_f^{\text{DLA}} = 1.715 \pm 0.004$, [11]). At low temperatures, on the other hand, the fractal dimension is much smaller, and closer to 1 ($D_f = 1.13 \pm 0.01$ at $T_r = 0$). That is, the lower the temperature, the stronger the screening effects of the branches, leading to an essentially digitated structure composed by fingers with very few side branches. At this respect, a significant difference with the case $d = 3$ is that now

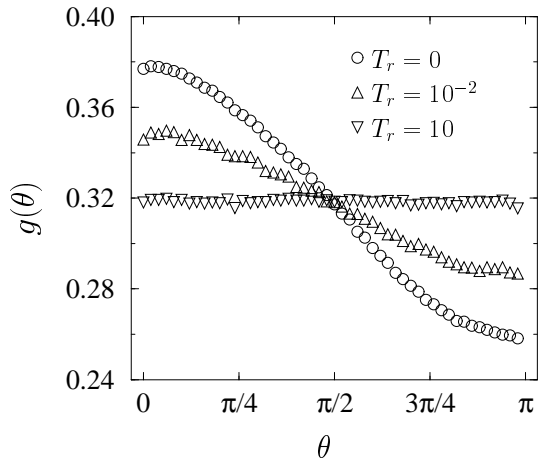


FIG. 3. Angular correlation function $g(\theta)$ in dipolar clusters in $d = 2$ for different values of the reduced temperature T_r .

clusters are always mutually opaque, $D_f^{(1)} + D_f^{(2)} > 2$, for all values of T_r .

Another remarkable feature of this system is the *ordering* induced by the dipolar interactions. A convenient way to measure this order is the angular correlation function $g(\theta)$ of the dipoles composing the cluster, defined as the fraction of all pairs of dipoles, irrespective of the position, forming a relative angle θ . This correlation function is shown in Fig. 3 for different temperatures. At high temperatures we observe that the system is completely disordered, with all orientations between dipoles being equally probable. More interestingly, at low temperatures we observe the emergence of an ordered phase, in which dipoles are parallel with high probability, while suppressing the anti-parallel (more energy costly) configurations. That is, there is an order-disorder transition (reflected in the angular correlation function g) between an ordered phase at the low-temperature limit (in the absence of any thermal disorder) in which the orientation of the dipoles is strongly correlated, and a disordered phase in the high-temperature limit, in which dipoles show an uncorrelated behavior, imposed by the intrinsic fractal geometry of the clusters.

The structures that we have shown in this section have been observed experimentally [14,15]. In the latter experiments, ferromagnetic particles of different sizes are transferred to a Langmuir monolayer at different pressures. The main observed feature is that the larger the diameter of the particles, the more digitated the emerging cluster. These experimental results can be interpreted by using our argument which is able to predict the shape of the clusters in terms of the reduced temperature. That equation indicates that, under those circumstances, the probability of a cluster to grow is much higher than the probability for splitting. Conversely, when the diameter of the particles is small, both probabilities equilibrate, resulting in denser circular compact aggregates, also in

accordance with experimental results.

III. CHAINING OF DIPOLAR PARTICLES ONTO A SUBSTRATE

In this Section we present results for a model of adsorption in which the adsorbing particles experience dipolar interactions. The irreversible adsorption of colloidal particles onto a solid surface is a very relevant subject, with plenty of practical and technological applications [16,17]. The basic models proposed so far in an attempt to understand the physics of adsorption are the random sequential adsorption model [18] and the ballistic model (BM) [19]. The BM model is a good approximation for the adsorption of large colloidal particles. In this model, particles arrive at the surface following straight vertical trajectories. When an incoming particle fails to reach the substrate directly, it is allowed to roll down over the previously adsorbed ones, until it reaches an equilibrium position. Particles eventually resting on the surface are adsorbed. Otherwise, they are rejected.

These models, and their subsequent generalizations, consider only very short range—usually hard-core—interactions. Here we will illustrate the profound effect of interparticle dipolar interactions in the adsorbed phase, for the case of ballistic adsorption.

A. Description of the algorithm

We consider the irreversible adsorption of dipolar particles that diffuse in a semi-infinite $d + 1$ -dimensional space and adsorb upon contact onto a boundary d -dimensional hyperplane (the substrate). In this case, the assembly of particles \mathcal{S} under consideration is the phase formed by all the particles adsorbed at given time, located at positions \mathbf{R}_i and carrying a rigid moment $\boldsymbol{\mu}_i$. Since we are considering an irreversible process, the adsorbed particles are fixed and cannot diffuse on top of the substrate. The algorithm used to simulate the random walk of the incoming particles is exactly as described in section II A, differing of course in the boundary conditions.

Simulations start with a clean substrate. Particles are released sequentially at random positions over a certain initial height h_{in} above the substrate, and with an initial random orientation $\boldsymbol{\mu}_0$. The particles perform a random walk until they either hit the substrate and become adsorbed or move away a distance larger than h_{out} . In this case, the particle is removed and a new one released. We have chosen the parameters $h_{\text{in}} = 15a$ and $h_{\text{out}} = 20a$, which are reasonable given the power-law decay of dipolar interactions (1). The rotational dynamics of the dipoles is the same as in the case of cluster aggregation, namely, dipoles relaxing at every accepted step. When a particle reaches a position very close to the

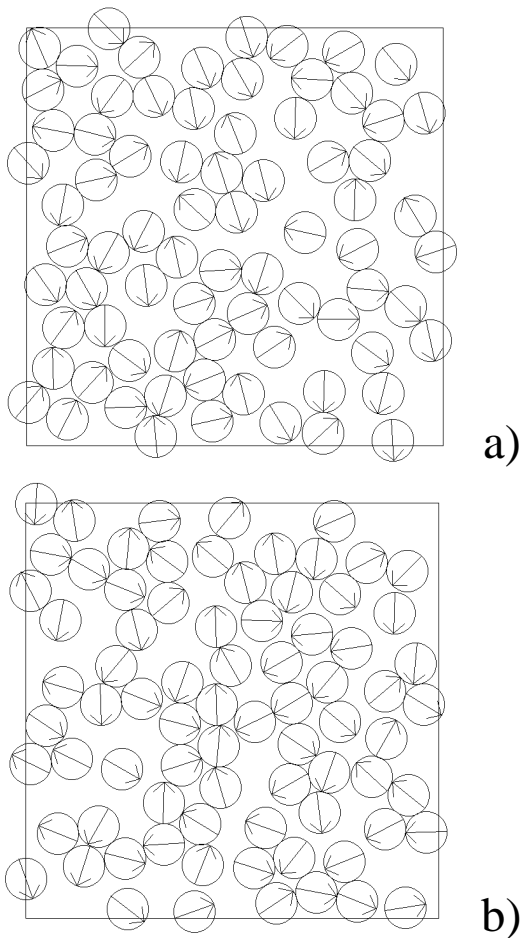


FIG. 4. Saturated configurations in $d = 2$, system size $L = 10a$. (a) Free BM, $T_r = \infty$. (b) With dipolar interactions, at $T_r = 0$. The particles extend out of the box to show the effect of periodic boundary conditions.

surface (less than one particle diameter a), it is attached to the substrate following the BM rules. This procedure assumes therefore the presence of a strong short-ranged interaction between substrate and particles, which overcomes dipolar interactions at very short distances. The newly adsorbed particles experience one last relaxation, and their moment does not change any more afterwards. The adsorbing surface has linear dimension L and we impose periodic boundary conditions in all directions but in the perpendicular to the plane. The system sizes considered in this work range between $L = 150a$ and $L = 250a$.

B. Numerical results in $d = 2$

Again, numerical simulations in $d = 2$ are very time-consuming and permit only to consider very small system sizes. In Figure 4 we have represented two typical saturated configurations, corresponding to the adsorption according to the rules of standard BM ($T_r = \infty$) and

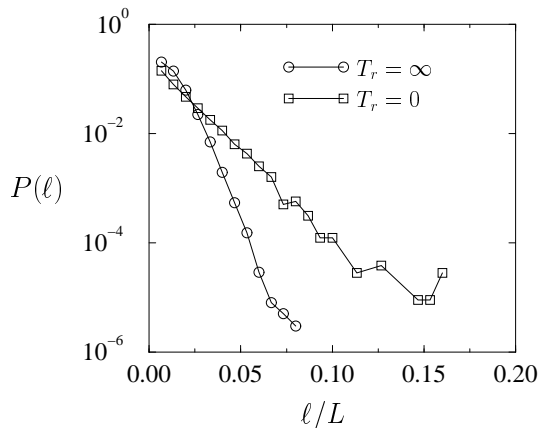


FIG. 5. Chain-length density function $P(\ell)$ for different values of the reduced temperature T_r , for dipolar adsorption in $d = 1$. System size $L = 250a$.

in the presence of dipolar interactions ($T_r = 0$). Inspection of these figures allows to conclude that the packing of the substrate is higher in presence of interactions. A numerical measure of the packing is given by the *jamming limit* θ_∞ , defined as the maximum fraction of the surface covered by particles at the saturation limit. Our simulations provide a value $\theta_\infty = 0.622 \pm 0.003$ for the dipolar adsorption at $T_r = 0$, whereas the standard BM ($T_r = \infty$) corresponds to $\theta_\infty^{\text{BM}} = 0.61048 \pm 0.00013$ [20]. This increase in the packing of the saturated surface can be traced back to the attractive interactions between the adsorbed phase and the incoming particles. In the case of standard free BM, the structure of the adsorbed phase is due exclusively to excluded volume effects: the already attached particles impede the adsorption of new particles at random positions, and allow only the occupation of empty spaces. This is essentially a random, disordering, effect. The presence of dipolar interactions, attracting the random walker to the surface, diminishes the excluded volume effects and leads to configurations of higher packing.

C. Numerical results in $d = 1$

By restricting the adsorption onto a line, we can explore more thoroughly the interplay between interactions and the disordering excluded volume effects. As we can conclude from examination of Fig. 4, the reason of the higher coverage is the larger tendency of dipolar particles to form connected structures at low temperatures. In $d = 1$ these connected structures are identified with chains. We therefore propose as a measure of order the chain-length density function $P(\ell)$, defined as the average number of chains of length ℓa , per unit length of substrate. From this function we can compute the remaining interesting properties of the adsorbed phase, like the jamming limit

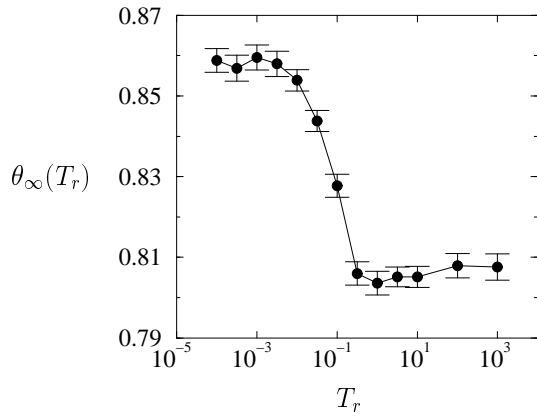


FIG. 6. Jamming limit θ_∞ as a function of the reduced temperature T_r , for dipolar adsorption in $d = 1$.

$$\theta_\infty = \sum_{\ell} \ell P(\ell). \quad (4)$$

In Figure 5 we have represented the chain-length density function for dipolar adsorption at $T_r = 0$ and $T_r = \infty$ (free BM). At high temperature we observe a very fast (super-exponential) decay of $P(\ell)$, indicative of a lack of any characteristic length; disorder has suppressed the formation of correlated chains in this case. At low temperatures, however, $P(\ell)$ decays exponentially, $P(\ell) \sim \exp(-\ell/\xi)$, with a well-defined correlation length (or average chain size) $\xi = 4.73 \pm 0.02$. Chains have now the possibility of growing very large, and a single chain is seen to cover more than 15% of the whole substrate.

Finally, we have plotted in Fig. 6 the jamming limit as a function of the reduced temperature T_r . At high temperature ($T_r = 10$) we recover the theoretical value $\theta_\infty^{\text{BM}} = 0.8079 \pm 0.0003$ [19]. On the other hand, at low temperatures the higher packing due to the chaining of the particles leads to a higher coverage, namely $\theta_\infty = 0.855 \pm 0.002$, which differs from the free case in about 6%, a notable variation in the context of adsorption phenomena. Note, moreover, the strong resemblance of Figs. 2 and 6, which depict analogous magnitudes in both models presented.

IV. CONCLUSIONS

The results presented in this paper render the following conclusions. The overall behavior of assemblies of magnetic particles is the result of the competition of factors of different nature: dipolar interactions, thermal disorder (Brownian motion) and screening (for aggregation) or excluded volume effects (for adsorption).

The concept of reduced temperature enables us to ascertain the global form of the clusters. A more precise analysis of the geometry of the structures, able to account for their local structure, needs however the use of fractal concepts, and in particular of fractal dimension. In the

cases we have discussed, magnetic particles may assemble basically into structures of effective $D_f = 1$, corresponding to the chaining process on a substrate mediated by excluded volume interactions, or into structures with values of D_f comprised in the interval $]1, 2[$, ranging from digitated to spherical clusters.

In the case of dipolar cluster aggregation, we have observed the existence of transitions between an ordered, or *quasi-ordered*, phase emerging at low values of the reduced temperature (and therefore comprising the low temperature and large particle size cases) and a disordered phase for high values of the reduced temperature. The low temperature phase is characterized by the existence of long-range correlations between dipoles. In the $d = 2$ case, our predicted results have been corroborated in experiments of aggregation performed on Langmuir monolayers. This technique has revealed to be a very useful tool in the characterization of the resulting two-dimensional structures.

Finally, it is worth pointing out that the existence of order at the mesoscopic level may have implications in the behavior of macroscopic quantities, such as the magnetization of the system.

ACKNOWLEDGMENTS

The work of R.P.S. has been supported by the European Network under Contract No. ERBFM-RXCT980183. J.M.R. acknowledges financial support by CICYT (Spain), Grant No. PB98-1258, and by the INCO-COPERNICUS programme of the European Commission under Contract No. IC15-CT96-0719.

-
- [1] J. M. Rubí and J. M. G. Vilar, J. Phys. C (in press).
 - [2] R. Pastor-Satorras and J. M. Rubí, Phys. Rev. E **51**, 5994 (1995).
 - [3] R. Pastor-Satorras and J. M. Rubí, Phys. Rev. Lett. **80**, 5373 (1998).
 - [4] T. Vicsek, *Fractal Growth Phenomena*, 2nd ed. (World Scientific, Singapore, 1992).
 - [5] P. Meakin, *Fractals, Scaling and Growth far from Equilibrium* (Cambridge University Press, Cambridge, 1998).
 - [6] T. A. Witten and L. M. Sander, Phys. Rev. Lett. **47**, 1400 (1981).
 - [7] P. Meakin, Phys. Rev. Lett. **51**, 1119 (1983).
 - [8] K. Kolb, R. Botet, and R. Jullien, Phys. Rev. Lett. **51**, 1123 (1983).
 - [9] D. A. Weitz and M. Oliveria, Phys. Rev. Lett. **52**, 1433 (1984).

- [10] J. D. Jackson, *Classical Electrodynamics*, 2nd ed. (John Wiley & Sons, New York, 1975).
- [11] S. Tolman and P. Meakin, *Phys. Rev. A* **40**, 428 (1989).
- [12] T. A. Witten, *Rev. Mod. Phys.* **70**, 1531 (1998).
- [13] V. M. Kaganer, H. Möhwald, and P. Dutta, *Rev. Mod. Phys.* **71**, 779 (1999).
- [14] G. Indivero, A. C. Levi, A. Gliozzi, E. Scalas, and H. Möhwald, *Thin Solid Films* **284–285**, 106 (1996).
- [15] S. Lefebure, C. Menager, V. Cabuil, M. Assenheimer, F. Gallet, and C. Flament, *J. Phys. Chem. B* **102**, 2733 (1998).
- [16] M. C. Bartelt and V. Privman, *Int. J. Mod. Phys. B* **5**, 2883 (1991).
- [17] J. Evans, *Rev. Mod. Phys.* **65**, 1281 (1993).
- [18] A. Rényi, *Sel. Trans. Math. Stat. Prob.* **4**, 203 (1963).
- [19] J. Talbot and S. M. Ricci, *Phys. Rev. Lett.* **68**, 958 (1992).
- [20] A. P. Thompson and E. D. Glandt, *Phys. Rev. A* **46**, 4639 (1992).